MORFEO Calibration Unit: optimization of the performances for the final design

Ivan Di Antonio, Gianluca Di Rico, Gabriele Rodeghiero, Angelo Valentini, Mauro Dolci, Benedetta Di Francesco

MORFEO Calibration Unit: optimization of the performances for the final design

Ivan Di Antonio*[a,c], Gianluca Di Rico[a,c], Gabriele Rodeghiero[b], Angelo Valentini[a,c], Mauro Dolci[a,c], Benedetta Di Francesco[a,c]

[a] INAF – Osservatorio Astronomico d'Abruzzo, Via Mentore Maggini, 64100 Teramo, Italy;
[b] INAF – Osservatorio di Astrofisica e Scienza dello Spazio, Via Gobetti 93/3, 40129 Bologna, Italy
[c] INAF-ADONI – Adaptive Optics National lab in Italy

*ivan.diantonio@inaf.it; phone +39 0861439706

ABSTRACT

The Calibration Unit of MORFEO, the Multi-conjugate adaptive Optics system of the Extremely Large Telescope, is a complex opto-mechanical subsystem used to project on the telescope focal planes a large number of high-quality light sources at different wavelengths, needed to run calibration, verification and test procedures on MORFEO. This subsystem will play a critical role not only during operations, but also during the Assembly, Integration and Test/Verification phase, both in Italy, when it will be used in Test Unit configuration, including a deformable mirror, and in Chile. This paper shows the progress in the re-design process started after the Preliminary Design Review, the performances improvement obtained from both the optical and mechanical points of view, and the path towards the Final Design.

Keywords: Adaptive Optics, calibration, beam splitter, homogeneity, ghosts, stray light, gravitational deformations, finite elements.

1. INTRODUCTION

MORFEO (Multi-conjugate adaptive Optics Relay For ELT Observations) is a post-focal adaptive optics module, based on Multi-Conjugate Adaptive Optics (MCAO). It is designed to enable high-angular resolution observations in the near-infrared by correcting in real-time the wavefront distortions due to atmospheric turbulence and other disturbances over a large Field of View (FoV). MORFEO will be firstly used by MICADO (Multi-AO Imaging CAmera for Deep Observations) [1], a near-infrared high-angular resolution imager, to compensate for aberrations and provide high-Strehl images within a FoV of nearly 1 arcmin. The MORFEO project is currently in ESO's phase C (Final Design): an overview can be found in [2] and [3]. The Calibration Unit (CU) will provide suitable light sources, simulating both Natural Guide Stars (NGS) and Laser Guide Stars (LGS), that will enable MORFEO to run calibration templates, such as Wavefront Sensors (WFS), Non-Common-Path Aberrations (NCPA) and tomographic reconstructor calibrations, as well as verification and test procedures, in standalone mode. Most of the daily or periodic calibrations, verifications and checks, will be performed thanks to this subsystem, thus minimizing the time spent calibrating on sky.
The CU sources are grouped into four typologies, according to their wavelengths, purposes and corresponding fed detector:

- NGS-REF sources → Mapping field distortions in R-band with well sampled PSFs
- NGS-LO sources → Calibrating low-order aberrations in H-band and simulating different anisoplanatic angles
- NGS-MIC sources → Calibrating NCPA between MICADO focal plane and NGS WFSs in H-band
- LGS sources → Calibrating LGS WFS probes at 589 nm.

2. PRELIMINARY DESIGN AND ITS CRITICALITIES

A detailed description of the CU preliminary design can be found in [4] and [5], while the revision process started after the Preliminary Design Review (PDR) is described in [6].
The PDR showed the adequacy of the overall solution but also highlighted some weaknesses and possible criticalities, to tackle and solve or at least mitigate during the project phase C (Final Design).

Here a list of the main areas identified as critical:

a) Cube beam-splitter (CBS)
   - Large size, to be even slightly increased due to manufacturing needs
   - Very tight manufacturing tolerances (surface irregularities, homogeneity)
   - It is the main ghosts-generator

b) Small clearance between optical and mechanical components
   - Impractical assembly and alignment
   - No space for baffles and vanes against stray light

c) LGS optics optimized for a single wavelength → Sensitiveness to small wavelength changes

d) Heavy "Telescope" optics (W, SM)

Other aspects to deal with are:

- Very low throughput, ghosts, massive presence of stray light
- Not-optimal gravity orientation of some optical components (BS1, BS2)
- Alignment strategy
- Mechanical structure construction

The main critical points are briefly described in the next section, as well as the solutions and mitigation strategies identified.

3. SOLUTIONS AND MITIGATION STRATEGIES

3.1 Cube Beam Splitter

The CBS was introduced to allow the full accessibility of the CU internal pupil plane. The review process has shown the impossibility of getting rid of this bulky component without a significant increase in optical aberrations, especially for the LGS channels. Moreover, the review highlighted the necessity to slightly increase the original cube size, from 140x140x140 mm^3 to 150x150x150 mm^3, to have more margin between the mechanical aperture and the clear aperture and allow the realization of protective chamfers.
The optical path length inside the CBS is ~300 mm. Even assuming the best available glass material, with a homogeneity of 1 ppm, it will translate into a wavefront error (WFE) of ~300 nm (P-V), with an expected value of 30-40 nm (rms), after focus subtraction. Preliminary inquiries with potential vendors for raw materials have shown that no supplier can guarantee a homogeneity level of 1 ppm in all directions, but only in one direction, with the other two at lower grades (from 2 to 4 ppm). Therefore, the overall WFE could be even higher than the previous estimate. Moreover, temperature changes (spatial gradients) will add their own contribution in a hardly-predictable way. Currently, the CBS material (Fused Silica) has quite a large sensitivity to thermal gradients via the change of the refractive index with temperature (*dn/dT*). BK7 can be considered a valid alternative (*dn/dT* about five times lower than that of Fused Silica), although its homogeneity grade is normally worse and its CTE is higher than that of Fused Silica.
In any case, the CBS cannot be removed from the optical system and it is one of the major contributors to the overall WFE, therefore it is particularly important to identify proper solutions and effective mitigation strategies. First of all, few 45° prisms shall be manufactured, and only the best ones shall be selected, cut and integrate along their best direction (highest homogeneity). Then, since the blank homogeneity induces a stationary WFE pattern, it will be possible to measure and compensated it by applying a correction map on the mirror positioned in the pupil plane (PM, Figure 1). It should be noted

that this compensation strategy is actually applicable to the fully integrated system, thus compensating more than just a single component.

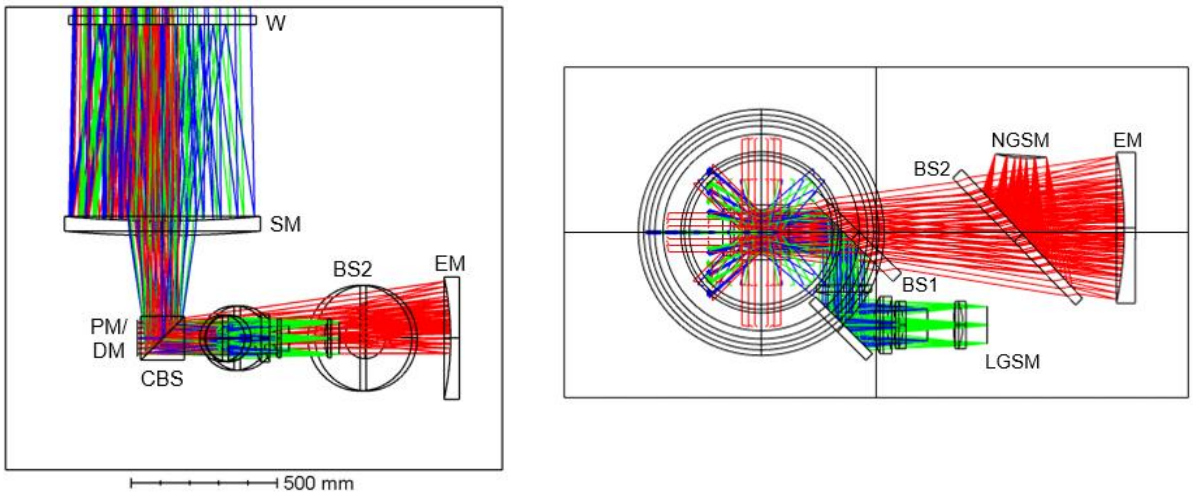

Figure 1. The new CU optical layout into the available space: front view (left), top view (right). As for the old layout: W lower surface and SM upper surface are semi-reflective, CBS, BS1 and BS2 are beam-splitters, EM is an elliptical mirror, NGSM and LGSM are the masks with the NGS and LGS sources, respectively, PM is the mirror positioned on the CU internal pupil, replaced by a Deformable Mirror (DM) in Test Unit mode. The red ray-tracing indicates the NGS optical path, the green and blue ones indicate the LGS optical paths (conjugated to 104 km and 150 km). The CU Folding Mirror (injecting the CU light sources into MORFEO) is not shown. Gravity goes from the top to the bottom of the front view.

3.2 LGS optics

The preliminary optical design of the LGS arm was optimized for a single wavelength (589 nm). Although this matches the monochromatic nature of the final laser beam, quasi-monochromatic sources will be used in the CU (bandwidth of ~10 nm). As shown in Figure 2, out of 589 nm, the LGS arm preliminary design shows a significant chromatic aberration (mostly lateral color), that increases the WFE and spreads the light over a larger spot, reducing the source intensity. The use of a monochromatic laser source is not optimal for different technical reasons, hence the only way to get rid of the chromatic aberration is a re-design of the LGS arm, in order to make it achromatic inside the defined LGS bandwidth, by introducing achromatic doublets in place of singlets.

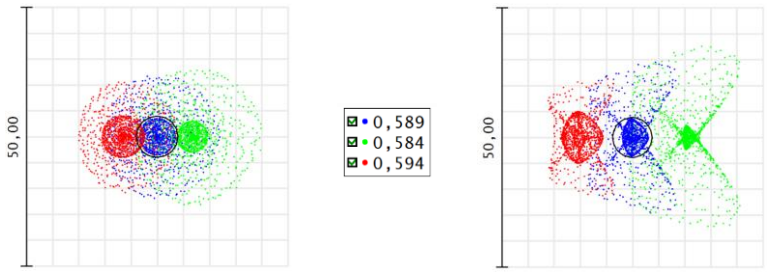

Figure 2. CU preliminary design performance: LGS spot diagrams over a 10 nm bandwidth. Source position on-sky: 45". Conjugation altitudes: 104 km (left), 150 km (right). The black circle is the Airy disk. Bar scale: 50 um

3.3 Mechanical issues

Both the semi-reflective flat Window (W) and Spherical Mirror (SM) are relatively large and heavy components (W with a diameter of 640 mm and a thickness of 60 mm, SM with a diameter of 670 mm and a thickness of 60 mm), fully suffering from gravity sag effect. While this effect can be minimized through a careful design of their opto-mechanical mountings, this will translate into mildly complex subsystems, requiring proper space and weight allocations. It is thus desirable to try to minimize their weight, by making both thinner, with a benefit also on the opto-mechanics. As a matter of fact, even if thinner elements will suffer more from gravitational deformations, a proper opto-mechanical design ensures that most of those deformations are axisymmetric (defocus, spherical aberration) so that they can be partially compensated during the system alignment. From the manufacturing point of view, there is a limit to the minimum thickness: this value is smaller for the flat window and larger for the spherical mirror.
Other two large optical components, namely the two plano beam-splitters BS1 and BS2, are oriented at 45° with respect to the gravity vector. For this reason, they suffer from asymmetric gravitational deformations, due to their elliptical shape, limited thickness and the need to have them attached along their periphery. The system would definitely benefit if the optical surfaces were parallel to the gravity vector.
Finally, the clearance between many opto-mechanical elements is very limited. This involves difficulties during the integration and alignment phases, as well as during the maintenance operations, increasing the possibility of collisions and thus the risk of damaging the optical components. There is also very little room to install baffles and vanes to prevent stray light, that is crucial in such an optical layout.

4. TOWARDS THE FINAL DESIGN

All the concerns described in the previous section claimed for an alternative optical layout. The optical and mechanical re-design has been performed in parallel in order to overcome most of the limitations of the preliminary design, without changing the overall optical concept, that the review confirmed to be the only possible, according to the available volume.

4.1 Optical design

The new optical layout is shown in Figure 1. The main changes with respect to the preliminary design are listed below:

- Different location of the optical components inside the available volume (distance SM-CBS, LGS arm folding direction) → Increase of the clearance
- Thickness of W and SM reduced to 30 and 50 mm, respectively → Weight reduction (~30 kg of glass saved)
- Increased CBS size: 150x150x150 mm^3
- Improved NGS beam collimation → No astigmatism induced by the plano Beam Splitters (BS1, BS2), possibility to place them in parallel
- BS1 and BS2 parallel and rotated by 90° along the horizontal axis → No gravitational deformations
- BS1 and BS2 wedged by ~1° → Improvement of off-axis NGS image quality, reduction of double-bounce ghosts (produced by the previous parallel plano surfaces placed on a collimated beam)
- LGS arm folded towards the elliptical mirror → Much more space available at the bottom, easier integration
- LGS lenses redesigned to be achromatic within the 584-594 nm band and to improve the nominal LGS image quality for extended sources and both conjugated altitudes.

In particular, the new LGS arm design (Figure 3) is based on one single lens (L1) and two achromatic doublets (L2, L3). Only one aspherical surface has been retained (there were two in the preliminary design). The second doublet (L3), added to improve both achromaticity and image quality, is stationary with the LGS mask (LGSM), moving jointly with it. Finally, the design has been optimized to provide larger tolerances.

The optical performances of the new design are shown in terms of spot diagrams on the CU exit focal plane (Figure 4 and Figure 5) and nominal WFE (Table 1). From a quick comparison with the NGS spot diagrams of the preliminary design (Figure 6), the image quality improvement is evident.

The quality of the CU exit pupil, in terms of pupil blur and distortion, is shown in Figure 7. The maximum blur (at the pupil edge and at the lowest wavelength) results to be ~0.95% of the pupil diameter (~0.55% considering the rms spot size), while the maximum distortion ~0.03%.

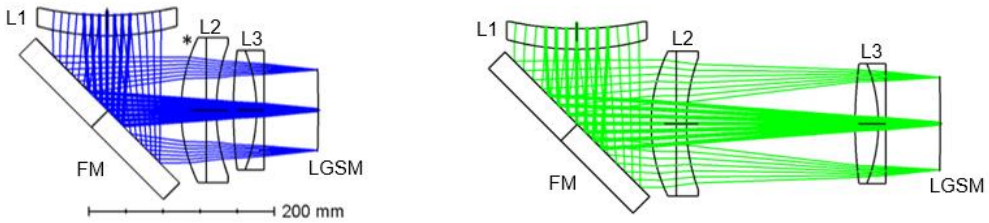

Figure 3. The new CU optical layout: LGS optics. Conjugation altitudes: 104 km (left), 150 km (right). The optical surface marked with the asterisk is aspherical. The doublet L3 moves jointly with the mask with the LGS sources (LGSM).

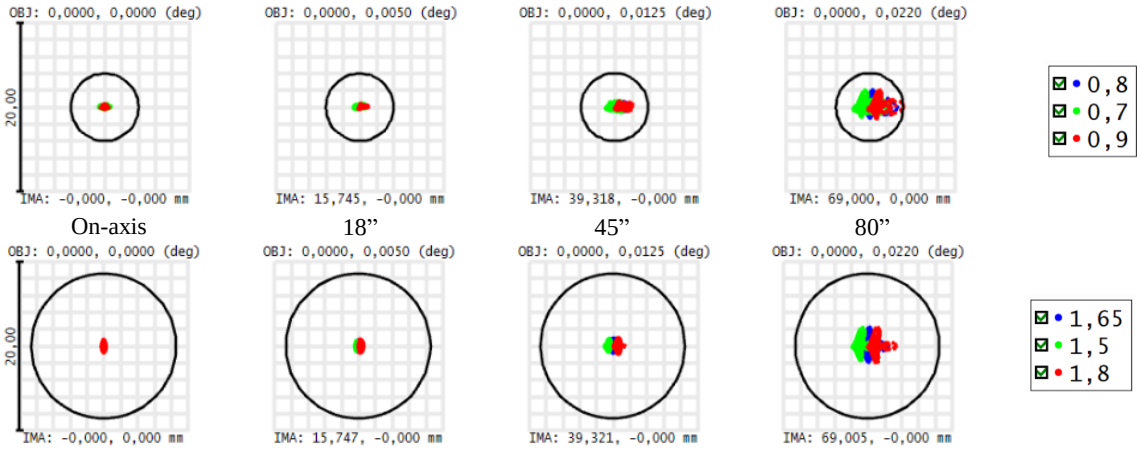

Figure 4. Performance of the new CU optical layout: NGS spot diagrams in R-band (top) and H-band (bottom) across the technical FoV. The black circle is the Airy disk at the shortest wavelength. Bar scale: 20 um

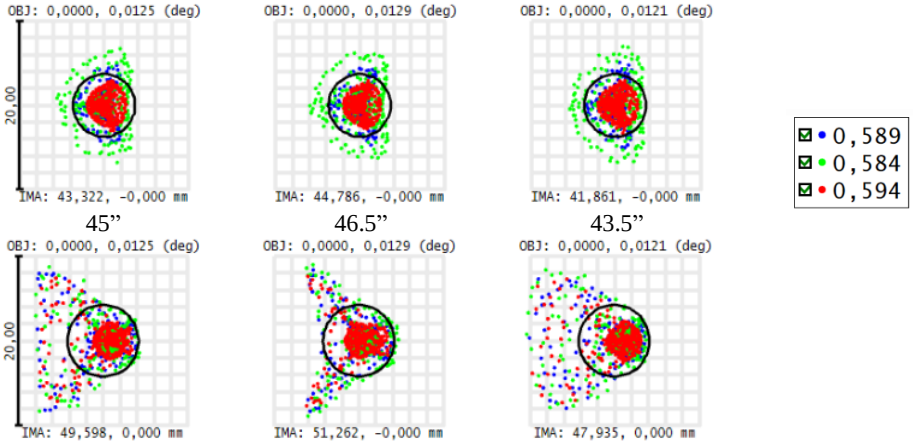

Figure 5. Performance of the new CU optical layout: LGS spot diagrams (sources are 3” in diameter, centered at 45”) @104 km (top) and @150 km (bottom). The black circle is the Airy disk at the shortest wavelength. Bar scale: 20 um

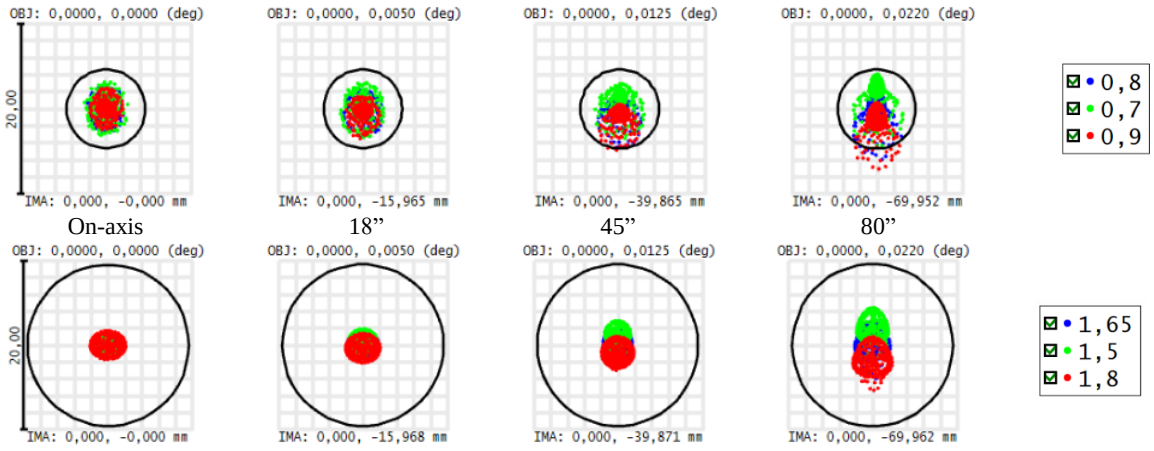

Figure 6. Performance of the old CU optical layout: NGS spot diagrams in R-band (top) and H-band (bottom) across the technical FoV. The black circle is the Airy disk at the shortest wavelength. Bar scale: 20 um

Table 1. Performance of the new CU optical layout: Nominal WFE (nm, rms), computed at the central wavelength (nm) of the band defined for each channel.

	NGS-REF	NGS-LO	NGS-MIC	LGS@104km	LGS@150km
Central wavelength	800	1650	1650	589	589
Preliminary design	16	26	28	37	40
New design	10	11	11	20	23

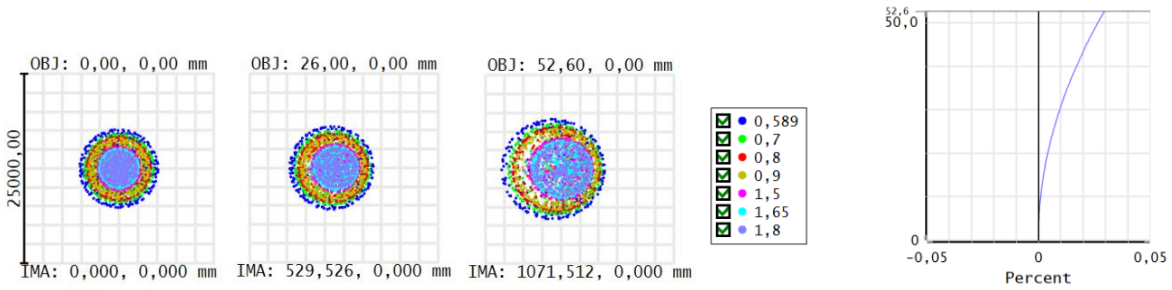

Figure 7. Performance of the new CU optical layout: pupil blur (left) and plot of pupil distortion (right) at different pupil points.

4.2 Mechanical design

The new optical design is driving the ongoing mechanical re-design. The overall tubular supporting structure has been retained, slightly modified to accomplish the new needs and solve most of the previous construction difficulties. It has been optimized in the tube sections thanks to a flexible finite element (FE) model (Figure 8), where the tubular structure has been modeled through “beam” elements and the non-structural elements have been replaced by their equivalent masses. The FE Analyses (FEA) performed to check the adequacy of the new mechanical design, as well as the verification criteria are summarized in Table 2. The results are shown in Table 3.

Table 2. Analyses and verification criteria applied to the CU simulations.

Analysis	Verification	Requirement / Criterion
Modal	Eigenfrequencies	First Eigenfrequency (f_1) > 21 Hz
Earthquake	Resistance to stresses induced by earthquake	Safety Factor (SF) > 1.5
Buckling	Buckling conditions	Min. Safety Factor (abs. value) > 10

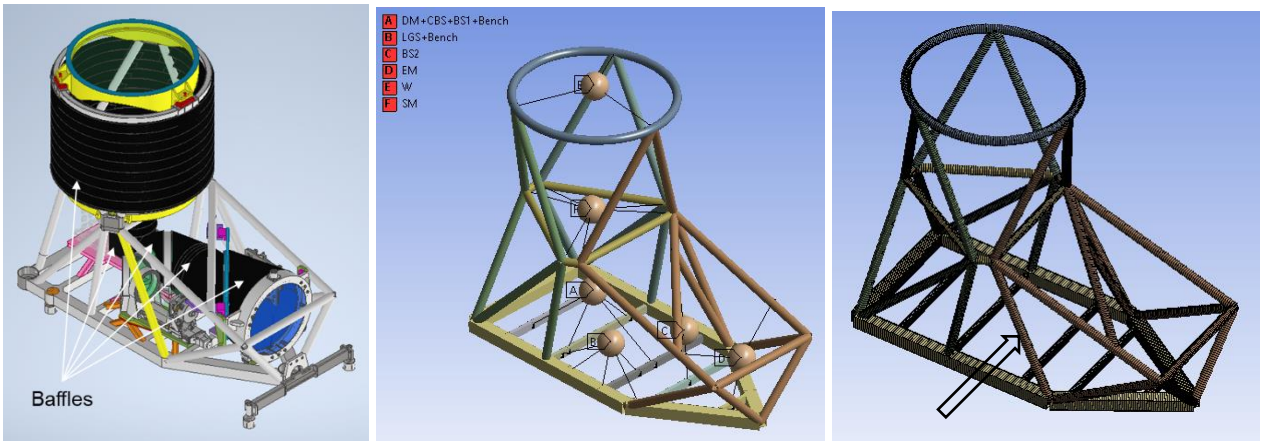

Figure 8. CU structure modelling: cad design (left), FE model (center), meshed model (right) ready for the simulations (performed with the software *Ansys*®). Masses in the model (kg): A=50, B=35, C=20, D=25, E=30, F=70, Tubes=60 (entity and distribution deriving from assumptions partly based on the preliminary design). The element indicated by the black arrow shall be removable to allow the mounting/dismounting of the LGS arm. The external cover of the CU is not represented.

Table 3. Results of the FEAs. The Earthquake Analysis Safety Factor (*SF*) is computed assuming the structural steel S235, as the ratio between the admissible stress (yield limit reduced by 30% in correspondence of a welded joint) and the maximum stress in the worst combination of equivalent earthquake accelerations.

Modal	Earthquake	Buckling
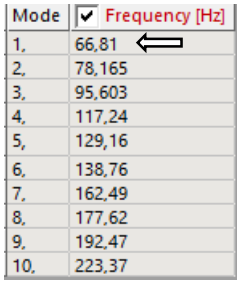	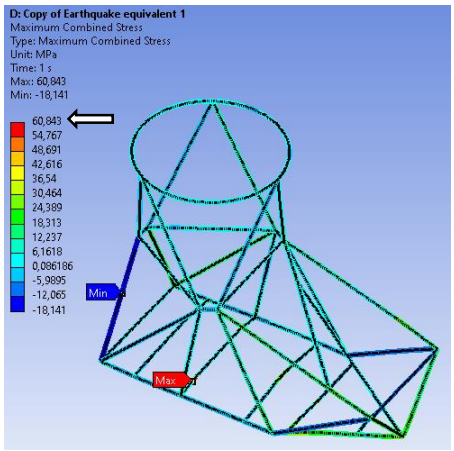	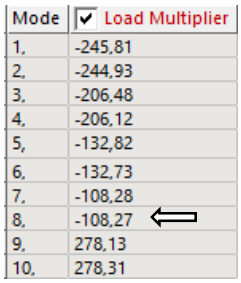
$f_1 = 67\ \text{Hz} > 21\ \text{Hz}$	$\sigma_{eq,max} = 61\ \text{MPa} \rightarrow\ SF = 2.7 > 1.5$	$SF\ \text{min} = 108 > 10$

4.3 Opto-mechanical design

In the new design the thickness of W and SM has been reduced, thus the gravitational deformation and the associated optical aberrations are higher. The opto-mechanics of these two components have to be carefully designed, in order to minimize the amount of non-axisymmetric deformations. The definition of type, amount, and disposition of the support points of the optics is propaedeutic to the design of their opto-mechanics, whose complexity increases with the number of support points, while the optical deformation decreases.
A trade-off analysis has been carried out on both W and SM to establish the best configuration. Three support configurations of increasing complexity have been analyzed, first through FEAs to derive the gravitational deformation of the optical surfaces, then imported into the optical model to compute the WFE associated with those deformations:

A) 6 isostatic axial support pads (3 bipods)
B) 6 isostatic axial support pads (3 bipods) + 3 adjustable spring supports (±10% of pre-load asymmetry)
C) 6 isostatic axial support pads (3 bipods) + 6 adjustable spring supports (3 bipods, ±10% of pre-load asymmetry)

The results of the FEAs carried out on W are shown in Table 4, where also histograms with the aberrations associated with the different deformations are reported. It is evident how the spherical aberration component (Z11) does not depend on the mounting configuration, but only on the optical aspect ratio and the supports radial position. The astigmatism (Z5, Z6) present in the configurations with spring-loaded pads is the result of the asymmetry defined in the pre-load (±10%). Configuration A is the only one where a significant component of hexafoil (Z28) is present.
The deformations of SM are not reported as they are qualitatively identical to those of W, simply scaled because SM is stiffer (similar diameter but larger thickness).

Table 4. Results of FEA carried out on W (620 mm of clear aperture, 30 mm of thickness): gravitational deformation (sag) and associated aberrations (Zernike coefficients, *Noll* notation) for each configuration.

Configuration A	**Configuration B**	**Configuration C**
Sag (m)	Sag (m)	Sag (m)
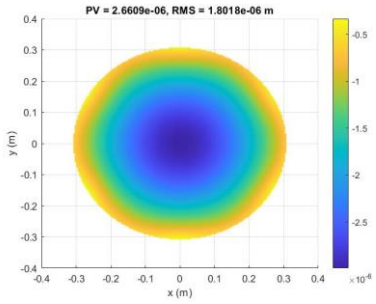	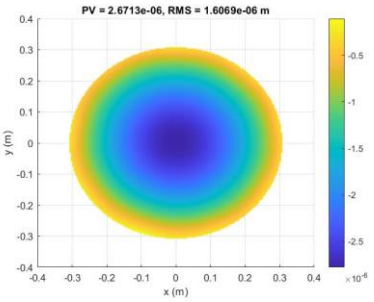	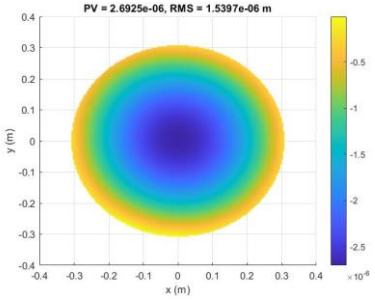
Sag (m) – NO piston/tip/tilt/focus	Sag (m) – NO piston/tip/tilt/focus	Sag (m) – NO piston/tip/tilt/focus
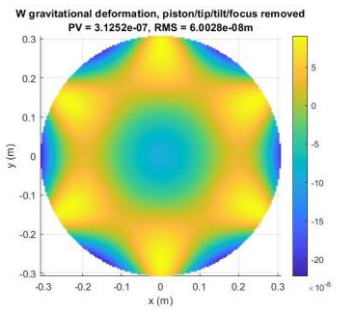	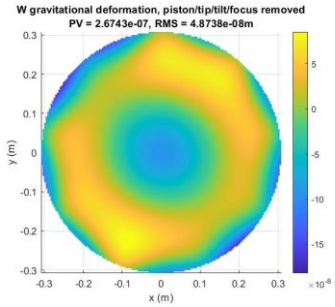	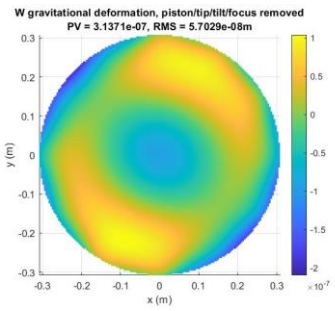

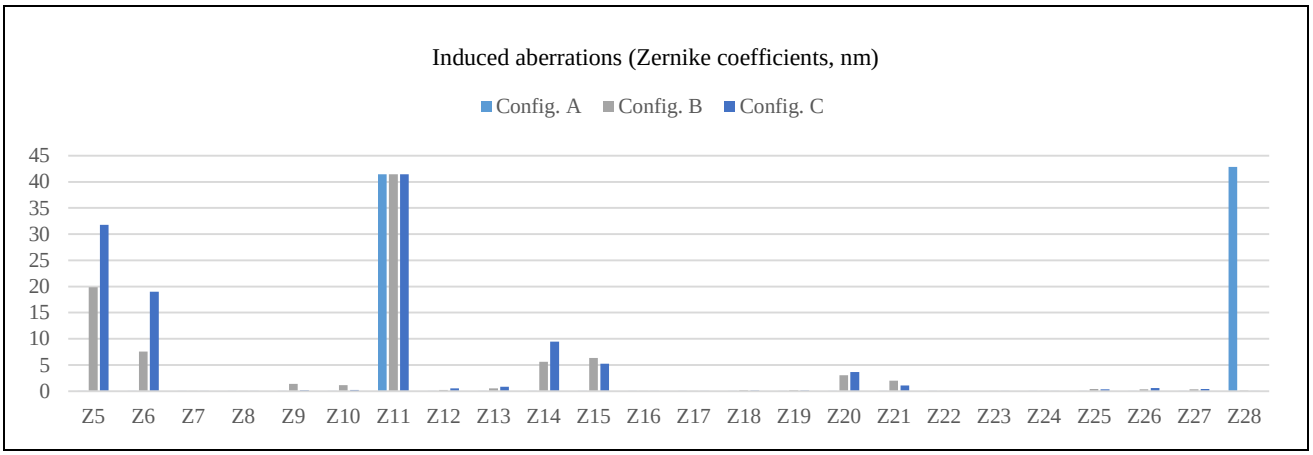

The impact of these induced aberrations has been analyzed for all the possible combinations of supports and for all the different optical channels of the CU. The most sensitive channel, as already known, turns out to be LGS@104km and the complete results (all possible combinations of support configurations) of induced WFE are shown only for this channel (Figure 9). The WFE introduced by the chosen combination is negligible for all the other channels. The plot of Figure 9 clearly shows that configuration C does not perform better than configuration B and that configuration A is not adequate for SM. The best combination results to be the configuration B for both W and SM.

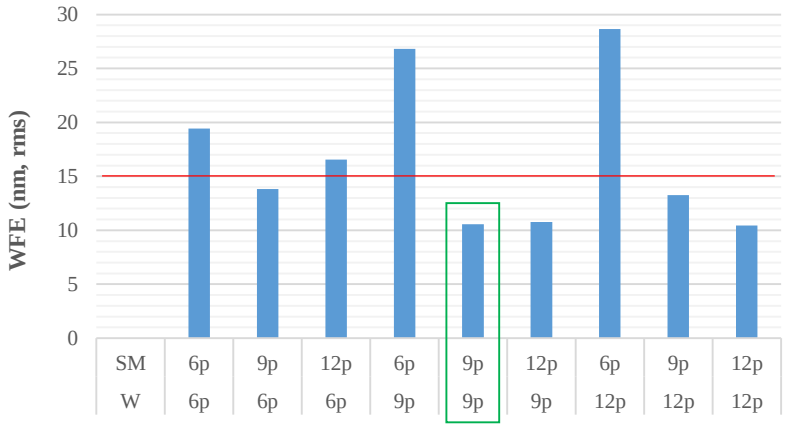

Figure 9. WFE (nm, rms) induced by W and SM gravitational deformation for the different support combinations. Naming: 6p = Config. A, 9p = Config. B, 12p = Config. C. A threshold of 15 nm has been considered and the best configuration is highlighted in green.

4.4 Ghosts and straylight

The intrinsic characteristics of the CU design is the presence of several semi-reflective surfaces, necessary to obtain such a compact layout. The obvious main drawback is the very low throughput, the presence of multiple ghosts and a massive presence of stray light.
With a proper sizing of the physical light sources, the problem of the low throughput has been solved. The light path design and relative computations performed for the preliminary design remain valid.
The CBS is the main ghost-generator. Figure 10 left shows the two main ghosts generated in correspondence of the CBS, one coming from the light back-reflected by the surface C (orange arrows) and the other from the light back-reflected by the surface E (red arrows). The non-sequential simulations performed on the preliminary design (Figure 10 center and

right), qualitatively still valid, indicate that an Anti-Reflection coating with a residual reflectivity ≤ 3% will damp the ghosts at a level ≤ 0.4% of the real PSF intensity. The analysis will be updated with the new optical design, anyhow we expect a lower ghost intensity, because the distance between surface C and the Pupil Mirror (PM) is 2 mm larger than that of the preliminary design, and this means that the ghosts defocus on the CU output focal plane will be slightly larger.

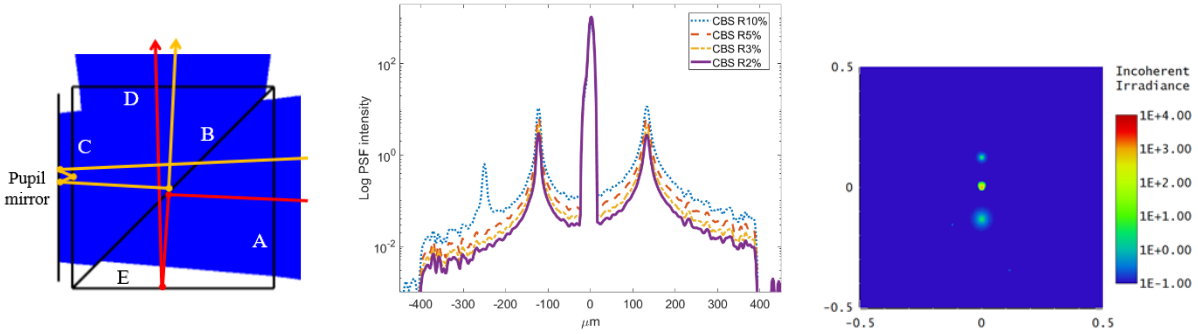

Figure 10. *(left)* Sketch with the indication of the main ghosts generated by the CBS. *(center)* Cross-Section of PSF and ghosts obtained from the non-sequential ray-tracing with different CBS glass residual reflectivity (Rn%): NGS ghosts lateral position and amplitude with respect to the real PSF. *(right)* Simulated high-resolution images of the NGS focal plane (1" FoV, R3%).

For what concerns the stray light, the design of baffles and vanes is ongoing. Figure 8 left shows the main baffles foreseen in the CU, that will likely be realized by welding of thin steel sheets, coated with black absorbent (>95%) paint. The tubular structure will also be coated with the same paint, while the opto-mechanics will be subjected to a burnishing process. The use of *Acktar*© sheets is an option, as well. Once the mechanical and opto-mechanical designs are developed in detail, a full non-sequential model with all the 3d models of the mechanics will be created, so that a reliable stray light analysis can be performed.

4.5 Alignment strategy

The optical and mechanical re-design also has taken into account the need to align the system as easily as possible. With the LGS arm now placed on the same horizontal plane of the NGS arm, it is possible to clearly identify two blocks for alignment purposes: the "Telescope" block and the "Optical Bench" block (Figure 11 left), with the LGS arm considered as a sub-block. This separation is enabled by the NGS collimated beam at the Pupil Mirror level, which provides an easy optical interface between the two blocks, alignable as standalone systems. The definition of the alignment plan is ongoing and will be the subject of a dedicated paper, also considering the experience meanwhile gained from the ongoing work on the CU paraxial prototype (PCUP), settled in Teramo lab (Figure 11 right). Actually, the prototype has been built considering the preliminary design and alignment strategy, but is flexible enough to be re-arranged in the final design configuration.

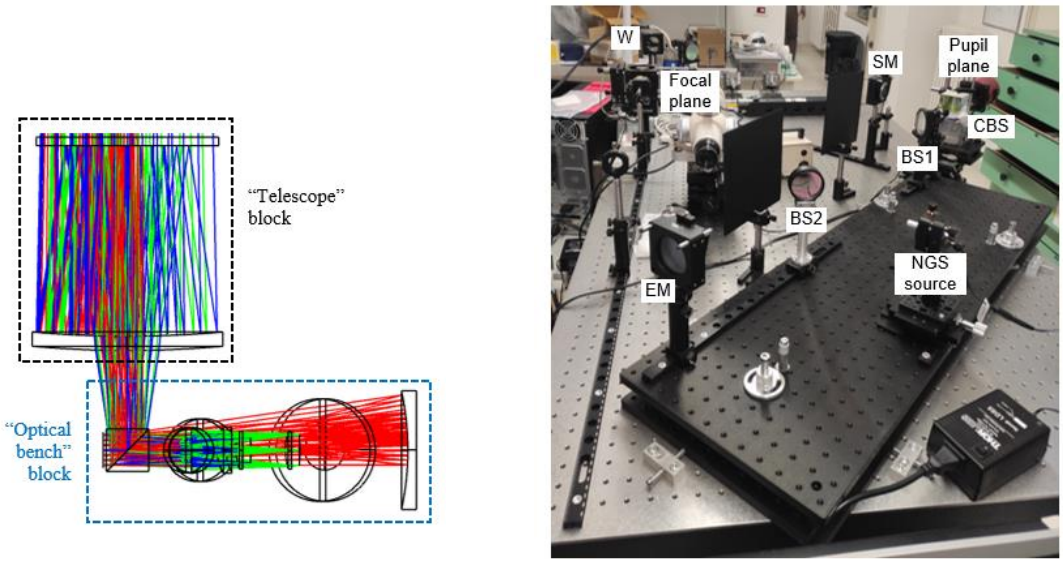

Figure 11. *(left)* CU conceptual division for alignment purposes. *(right)* CU paraxial prototype (only the NGS path is reproduced, 2-inches optics are used), settled in Teramo lab to simulate and get familiarity with the alignment procedure.

5. CONCLUSIONS

The Calibration Unit of MORFEO has entered the Final Design phase. A deep review process made it possible to solve most of the criticalities of the preliminary design, thanks to an optical re-design of the system. The mechanical re-design is ongoing: once completed, it will be possible to perform complete ghosts and straylight analyses. The definition of the alignment plan is also ongoing, supported by the work performed in the lab on the CU prototype. The refinement of the WFE budget breakdown is ongoing, according to the new optical layout, the updated tolerance analysis and some information got from the optics manufacturers. The overall WFE budget is very tight, dominated by the CBS contribution and by the contribution coming from the manufacturing tolerances of the other optical elements. The implementation of a compensation strategy (Pupil Mirror final polishing after measurement of the system nominal aberrations) could be necessary.

REFERENCES

[1] Davies, R., et al.: "MICADO: The Multi-Adaptive Optics Camera for Deep Observations", The Messenger, vol. 182, p. 17-21 (2021)
[2] Ciliegi, P., et al.: "MAORY/MORFEO @ELT: general overview up to the preliminary design and a look towards the final design", Proc. SPIE, 1218514 (2022)
[3] Busoni, L., et al.: "MORFEO enters final design phase", this conference
[4] Di Rico, G., et al.: "MAORY/MORFEO@ELT: Calibration Unit overview", Proc. SPIE, 121855F (2022)
[5] Di Antonio, I., et al.: "The calibration and test unit of MAORY/MORFEO: analyses and performance evaluation", Proc. SPIE, 121855G (2022)
[6] Di Rico, G., et al.: "MORFEO Calibration Unit: towards the final design", this conference